

# Electric field-induced resistance changes at low temperature on a Cr<sub>2</sub>O<sub>3</sub>/ultra-thin (La,Sr)MnO<sub>3</sub> magnetic hetero structure

Takeshi YOKOTA,<sup>†</sup> Shotaro MURATA, Shinya KITO and Manabu GOMI

Materials Science and Engineering, Nagoya Institute of Technology,  
Gokiso-cho, Showa-ku, Nagoya-shi, Aichi, 466-8555

We have investigated the relationships between electric field-induced resistance change and the magnetic properties of the Cr<sub>2</sub>O<sub>3</sub>/ultra-thin La<sub>0.7</sub>Sr<sub>0.3</sub>MnO<sub>3</sub> (LSMO) magnetic hetero structure. The LSMO with a thickness of 40 nm has two transition temperatures, the ferromagnetic Curie temperature of 312 K and the spin-glass temperature of 180 K. Resulting from the magnetic properties, the exchange interaction in the Cr<sub>2</sub>O<sub>3</sub>/LSMO behavior below 180 K differed from that below 312 K. With the application an electric field on the Cr<sub>2</sub>O<sub>3</sub> gate, the resistance of LSMO film was changed. This resistance change is most likely due to the magnetic state of LSMO and the interface interaction between the Cr<sub>2</sub>O<sub>3</sub> and LSMO film

©2009 The Ceramic Society of Japan. All rights reserved.

Key-words : Magneto-electric effect, Exchange bias, Magnetic properties, Electric properties, Spin glass

[Received November 6, 2008; Accepted April 16, 2009]

## 1. Introduction

The phenomena of colossal magneto-resistance (CMR) materials expressed in manganite perovskite materials have attracted attention with regard to their potential use in new spintronics devices. The resistance changes of these materials are approximately 1000%, which is larger than that of general magnetoresistance effects such as the giant magnetoresistance effect.<sup>1,2)</sup> This is generally explained by the double exchange interaction via spin-polarized conduction electrons. On the other hand, magneto-electric (ME) effects have also received attention because the magnetic or dielectric properties can be controlled by an external electric or magnetic field.<sup>3,4)</sup> In the present study, we focused on Cr<sub>2</sub>O<sub>3</sub>, which shows the antiferromagnetic (AF) properties of ME materials.<sup>5,6)</sup> If we produce a magnetic hetero structure using Cr<sub>2</sub>O<sub>3</sub>, we can control its magnetic configuration through exchange coupling to adjacent ferromagnetic (FM) films by the use of an ME effect without an external magnetic field. We have previously reported an exchange interaction on a Cr<sub>2</sub>O<sub>3</sub>/(La, Sr)MnO<sub>3</sub>(LSMO) (AF/FM) hetero structure.<sup>7)</sup> In the case of LSMO film with a thickness of 40 nm, the film shows two magnetic transition temperatures that correspond to the ferromagnetic Curie temperature and the spin-glass temperature, respectively. The exchange interaction behaviors of the samples were found to differ according to the specific magnetic properties in each magnetic state. These differences in magnetic properties can be useful for investigation of the electric field resistance changes originating from the interfacial magnetic interaction changes due to the ME effect. Hence, in the present study we investigated the relationships between the electric field-induced resistance change and the magnetic properties of LSMO.

## 2. Experimental procedure

The Cr<sub>2</sub>O<sub>3</sub>/LSMO hetero structure was prepared using the radio-frequency (RF) magnetron sputtering method. Cr<sub>2</sub>O<sub>3</sub> and

stoichiometric LSMO sintered ceramics were used as the target. SrTiO<sub>3</sub> substrate was used as a substrate. The substrate was annealed at 1000°C for 3 h in oxygen atmosphere to obtain a step and terrace structure. The base pressure before introducing the sputtering gas was  $3.0 \times 10^{-4}$  Pa, and the gas pressure during deposition was  $8.0 \times 10^{-1}$  Pa. The gas used was a mixture of Ar and O<sub>2</sub>, and the ratios for LSMO were 9:1. The LSMO film with the thickness of 200 nm was deposited at 400°C. Since as-deposited LSMO did not show ferromagnetic properties due to the low growth temperatures, the samples were annealed at 900°C for 10 h in atmosphere. Then, Cr<sub>2</sub>O<sub>3</sub> with the thickness of 200 nm was deposited at 400°C. The gas used was a mixture of Ar and O<sub>2</sub>, and the ratios for Cr<sub>2</sub>O<sub>3</sub> were 16:1. Pt was used as a top gate electrode with a size of 700 μm. Au was used as a source-drain electrode. The drain-source length was 700 μm. The magnetic properties of the sample were measured using a Superconducting Quantum Interface Device (SQUID). A magnetic field of 500 Oe was used as a measurement field applied parallel to the film's surface, corresponding to the saturation magnetic field of LSMO. In order to investigate the interface magnetic properties, *M-T* measurements after field cooling (FC) with a magnetic field of 0.5 T were also performed. The structural analysis of the films was performed with an X-ray diffract meter (XRD) using Cu Kα radiation and Reflected High Energy Electron Diffraction (RHEED). The surface morphology was measured using an Atomic Force Microscope (AFM). The electric properties at low temperature were measured using a cryostat system (Nagase PS25SR). The effect of electric field on source-drain resistance of LSMO was evaluated by applying an electric field to the Cr<sub>2</sub>O<sub>3</sub> gate. The electric field induced resistance change (*ER*) was defined as  $ER = (R_E - R_0) \times 100/R_0$ , where *R*<sub>0</sub> and *R*<sub>E</sub> is the drain-source resistance at zero field and at a certain field, respectively.

## 3. Results and discussion

### 3.1 Structural analyses

Figure 1(a) shows the XRD pattern of the LSMO film with a thickness of 40 nm. The insets show the enlarged view from 22° to 24° and the RHEED pattern of the sample. Figures 1(b) and

<sup>†</sup> Corresponding author: T. Yokota; E-mail: yokota.takeshi@nitech.ac.jp

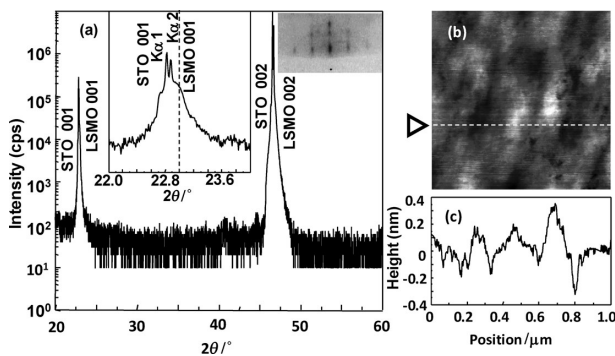


Fig. 1. (a) shows the XRD pattern of the sample. The insets show the enlarged view from  $22^\circ$  to  $24^\circ$  and the RHEED pattern of the sample. (b) and (c) show the AFM image and the surface profile along the dotted line in this image, respectively.

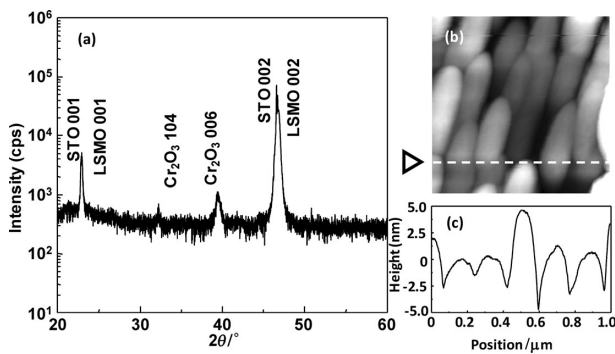


Fig. 2. XRD pattern of  $\text{Cr}_2\text{O}_3$  film deposited on the LSMO. (b) and (c) show the AFM image of the  $\text{Cr}_2\text{O}_3$  film and the surface profile along the dotted line in this image, respectively.

(c) shows the AFM image and the surface profile along the dotted line in this image, respectively. All diffraction patterns were identified as the  $\text{SrTiO}_3$  ( $K\alpha_1$  and  $K\alpha_2$ ) and the LSMO, respectively. The unknown sub peaks observed at  $22.7^\circ$  were originated from substrate, because these peaks were observed even at a virgin  $\text{SrTiO}_3$  substrate measured using our XRD system. The RHEED patterns revealed that the sample was epitaxially grown on the substrate. The AFM image and surface profile also revealed that the sample surfaces were smooth. The root-mean square (RMS) roughness of the sample was approximately 0.5 nm. **Figure 2** shows the XRD pattern and surface morphology of  $\text{Cr}_2\text{O}_3$  film deposited on the LSMO.  $\text{Cr}_2\text{O}_3$  film has 006 oriented polycrystalline structures. Judging from the RMS roughness of 5 nm, the sample was smooth enough to uniformly apply the voltage on the  $\text{Cr}_2\text{O}_3$  gate.

### 3.2 Magnetic properties

**Figure 3** shows the temperature dependence of magnetization ( $M$ - $T$ ) curves of the sample measured using a SQUID magnetometer. The  $M$ - $T$  without an FC (ZFC) curve has two transition temperatures of 312 K and 180 K. The FC and ZFC magnetizations have the same value above 180 K, but below 180 K there is a remarkable difference between the ZFC curve and FC curve up to the minimum temperature of measurement. The transition temperature of 312 K corresponded to the paramagnetic to ferromagnetic transition temperature ( $T_c$ ).<sup>8,9)</sup> In contrast, the transition temperature of 180 K corresponded to the spin-glass

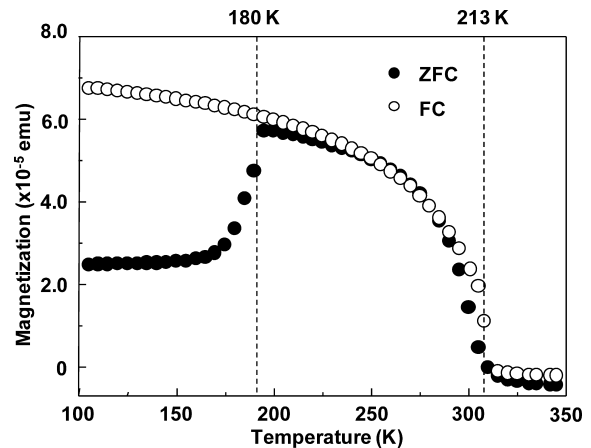


Fig. 3. Temperature dependence of magnetization of sample with zero field cooling (ZFC) and field cooling (FC): Field cooling was performed with a magnetic field of 0.5 T.

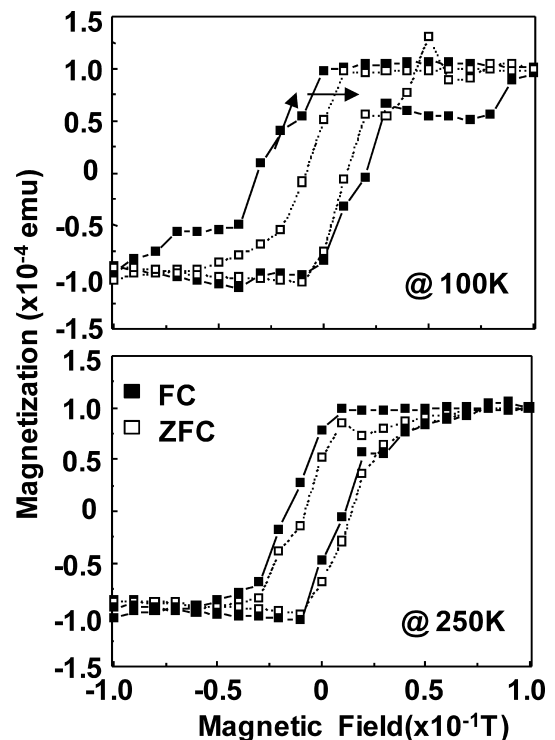


Fig. 4. Magnetization curves of sample with ZFC and FC measured at 100 K and 250 K.

temperature, judging from the differences between the ZFC and FC curves.<sup>10)</sup> **Figure 4** shows the magnetization curves measured at 100 and 250 K, which have different magnetic properties, respectively. The magnetization ( $M$ - $H$ ) curves were also measured after the FC process. A hysteresis shift in the  $M$ - $H$  curve was observed only at 250 K. The coercive force of the sample at 100 K became wider and showed steps after undergoing the FC process, as indicated by the arrow in Fig. 4. This phenomenon can be explained by spin-glass behavior. Spin glass basically has a non-periodic ground state and a complicated configuration space with many “valleys”.<sup>11)</sup> The FC and ZFC processes cause the stable spin state to change from one ground state to another ground state. In our system, the spin-glass state might be pro-

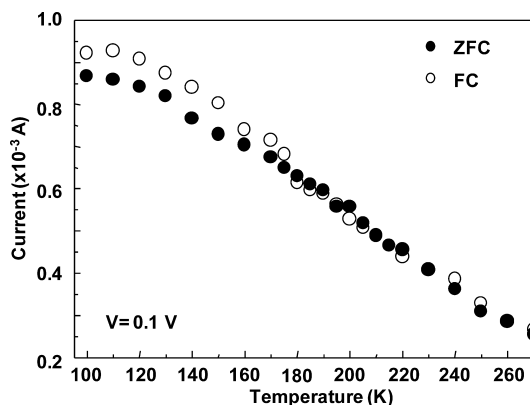


Fig. 5. Temperature dependence of current measured at 0.1 V of the sample with FC and ZFC.

duced by the conflict between crystal magnetic anisotropy and shape anisotropy.<sup>7)</sup> If we can apply a sufficiently large magnetic field to align all ferromagnetic spins, a stable magnetic state can be produced and frozen due to the spin-glass interaction. This result explains why the coercive force becomes wider. Furthermore, even if we can produce one magnetic domain state by administering the FC process, the domain wall motion will be pinned at the interface of the magnetic domain with a different anisotropy, thus causing a step in the  $M-H$  curve.

### 3.3 Electric properties

The temperature dependence of current measured at 0.1 V in a sample with FC and ZFC is shown in Fig. 5. The current values also showed differences below 180 K, likely due to the spin-glass nature. After the FC process, the magnetic spins were aligned and frozen along the magnetic field direction of the FC process. In contrast, the magnetic spins of the ZFC sample were random and frozen below 180 K. Since electrons are scattered by each frozen spin, the current values of the ZFC sample were decreased.

ER were investigated at 100 K and 250 K. The resistance change behaviors with the FC process were also investigated. First, we made sure that the leakage current of the  $\text{Cr}_2\text{O}_3$  gate did not affect the current of the LSMO channel. The leakage current was less than approximately  $1 \times 10^{-7}$  A, and the range of changes in current was approximately  $1 \times 10^{-5}$  A. As such, the leakage current of  $\text{Cr}_2\text{O}_3$  can be considered to be negligible. These results are shown in Fig. 6. The FC-ER at 100 K showed negative changes below the electric field of 5 kV/cm, and then the values changed to positive. The changes values of the FC sample are larger than those of ZFC sample within each of the gate voltages. These behaviors can be explained by the ME effects of  $\text{Cr}_2\text{O}_3$  film. Originally, the ZFC sample has a random frozen spin state. By application of the electric field, however, an induced magnetic moment originating from the ME effects can break the frozen state. Therefore, both the ZFC and FC resistances increased with increases in the external magnetic field. The differences between the ZFC and FC are due to differences between the frozen state, which is a random frozen spin state, and the ferromagnetic frozen state, respectively. FC-ER should be larger than ZFC-ER because the change from the aligned spin state to a random state was larger than that from the random spin state to a random spin state. In addition, the existence of the exchange bias field in the FC sample was another possible cause of the ER differences. The induced mag-

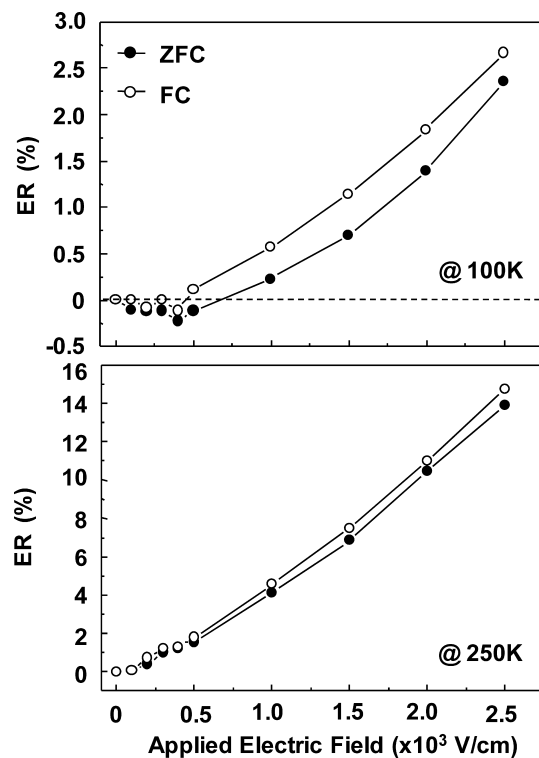


Fig. 6. Electric field-induced resistance changes (ER) of the sample with ZFC and FC are measured at 100 K and 250 K.

netic moment caused by the ME effects also breaks the exchange interaction. In any case, we can expect an increase in the resistance. Although we have not yet determined the physical origin of the negative resistance change below 5 kV/cm, we suppose that the behavior was also due to the ME effects of  $\text{Cr}_2\text{O}_3$ . During the process from the random spin state to a random spin state, the spins might be slightly aligned along the induced magnetic moment direction. The ER was also observed at 250 K. But the changes values were larger than those at 100 K. These results supported the explanation given above. Although there is no magnetic state difference between the ZFC and FC, there is a resistance difference. This difference could be due to the existence of an exchange bias. In addition, the ER was due to the ME effects. Since ME susceptibility is the largest at approximately 250 K,<sup>5)</sup> the turnability of the resistance by the electric field should be large.

### 4. Conclusions

We investigated the relationship between electric field-induced resistance change and the magnetic properties of LSMO. LSMO had a ferromagnetic Curie temperature of 312 K and a spin-glass transition temperature of 180 K. The exchange interactions between  $\text{Cr}_2\text{O}_3$  and LSMO changed depending on the magnetic properties of LSMO. By application of an external electric field on the  $\text{Cr}_2\text{O}_3$  gate, the resistance of LSMO was changed. The ER ratio and the differences in ER between the ZFC and FC revealed that this ER was more likely due to the magnetic state tuning of LSMO and the exchange tuning between the  $\text{Cr}_2\text{O}_3$ /LSMO interface by the ME effects.

**Acknowledgments** This research was supported in part by a grant from the Grant-in-Aid for Young Scientists (B) (20760197).

## References

- 1) S. Okamoto, S. Ishihara and S. Maekawa, *Phys. Rev. B*, **61**, 451 (2000).
- 2) C. N. R. Rao, A. R. Raju, V. Ponnambalam, S. Parashar and N. Kumar, *Phys. Rev. B*, **61**, 594 (2000).
- 3) N. Nur, S. Park, P. A. Sharma, J. S. Ahn, S. Guha and S-W. Cheong, *Nature*, **429**, 392 (2004).
- 4) J. Wang, J. B. Neaton, H. Zheng, V. Nagarajan, S. B. Ogale, B. Liu, D. Viehland, V. Vaithyanathan, D. G. Schlom, U. V. Waghmare, N. A. Spaldin, K. M. Rabe, M. Wuttig and R. Ramesh, *Science*, **299**, 1719 (2003).
- 5) E. Kita, A. Tasaki and K. Siratori, *Jpn. J. Appl. Phys.*, **18**, 1361 (1979).
- 6) T. Yokota, T. Kuribayashi, M. Gomi, T. Shundo and Y. Sakakibara, *Adv. Mater. Res.*, **11–12**, 133 (2006).
- 7) T. Yokota, T. Kuribayashi, S. Murata and M. Gomi, “Electroceramics in Japan XI,” Key Engineering Materials, in press.
- 8) Y. Tomioka, A. Asamitsu, H. Kuwahara, Y. Morito and Y. Tokura, *Phys. Rev. B*, **53**, R1689 (1996).
- 9) M. Nii, T. Oka, S. Yoshimura, H. Asano and M. Matsui, *J. Mag. Soc. Jpn.* **31**, 333–337 (2007).
- 10) K. Binder and A. P. Young, *Rev. Mod. Phys.*, **58**, 801 (1986).